nanomaterials

MDPI

Article

A Novel Bi_2MoO_6/ZIF-8 Composite for Enhanced Visible Light Photocatalytic Activity

Yu Xia [1], Shao-ke Shang [1], Xie-rong Zeng [1], Ji Zhou [2] and Ya-yun Li [1,*]

[1] Shenzhen Key Laboratory of Special Functional Materials & Shenzhen Engineering Laboratory for Advance Technology of Ceramics, College of Materials Science and Engineering, Shenzhen University, Shenzhen 518060, China; 2172341411@email.szu.edu.cn (Y.X.); 2172341466@email.szu.edu.cn (S.-k.S.); zengxier@szu.edu.cn (X.-r.Z.)

[2] State Key Laboratory of New Ceramics and Fine Processing, School of Materials Science and Engineering, Tsinghua University, Beijing 100084, China; zhouji@tsinghua.edu.cn

* Correspondence: kittyli@szu.edu.cn

Received: 3 March 2019; Accepted: 29 March 2019; Published: 4 April 2019

Abstract: A series of novel Bi_2MoO_6/zeolitic imidazolate framework-8 (ZIF-8) photocatalysts have been successfully fabricated through a facile self-assembly process. X-ray diffraction (XRD), scanning electron microscopy (SEM), UV-vis spectrophotometry, and X-ray photoelectron spectroscopy (XPS) characterized pure Bi_2MoO_6, pure ZIF-8, and a series of Bi_2MoO_6/ZIF-8 composites. The result indicated that, when compared with pure Bi_2MoO_6, the composite of Bi_2MoO_6/ZIF-8 exhibited excellent photocatalytic performance for the degradation of methylene blue (MB) under visible light. Moreover, the Bi_2MoO_6/ZIF-8-3 composite (the molar ratio of Bi_2MoO_6 to 2-MI is 3:3) has optimum photocatalytic performance because of the suitable amount of ZIF-8 decorated on the flower-like Bi_2MoO_6. The enhanced photocatalytic activity is probably due to the introduction of ZIF-8, which will promote the separation of electron–hole pair and the surface morphology. Benefitting from the diversity of the MOF species (ZIF-8 is one of them), this composing strategy of Bi_2MoO_6/MOF composite would provide new insight into the design of highly efficient visible light photocatalysts.

Keywords: Bi_2MoO_6; ZIF-8; photocatalysis; morphology

1. Introduction

Photocatalytic materials, especially semiconductor photocatalysts, have attracted a lot of attention in recent years due to the world-wide environmental problems, such as the water pollution [1–3]. However, as most semiconductor photocatalysts, such as TiO_2, cannot utilize visible light and respond to other visible lights, except ultraviolet light, because of a wide band gap, the photocatalytic activity of them was reduced [4]. Therefore, for the effective use of visible lights, the semiconductor photocatalyst should be able to respond to all visible lights and its band gap should be within a suitable range.

Bismuth molybdate (Bi_2MoO_6) is a typical Aurivillius oxide. When compared with the titanium dioxide, the Bi_2MoO_6 has a smaller forbidden band width (about 2.7 eV). As a result, it has a better photocatalytic activity within the visible range [5]. As is known to all, the morphology of the semiconductor photocatalyst plays a vital role in photocatalysis process [6]. Bi_2MoO_6 has a variety of morphologies that have been synthesized [7,8], among which the hierarchical flower-like Bi_2MoO_6 spheres have attracted a lot of attention with their super photocatalytic performance. In addition, the catalytic efficiency of the semiconductor photocatalyst can be greatly improved by increasing the number of photogenerated electron-hole pairs, inhibiting the recombination of photogenerated electron-hole pairs and increasing the reaction sites of the catalyst with the reactants. The photocatalytic

activity of the Bi_2MoO_6 photogenerated electron-hole pairing ratio is relatively high. To further improve the photocatalytic activity of Bi_2MoO_6, many feasible studies have been conducted, such as ion doping [9], surface noble metal deposition [10], and compounding of semiconductor photocatalysts [11]. However, there is still much room for the exploration of the potential of bismuth molybdate-based as a photocatalyst material.

Metal-organic frameworks (MOFs) is a kind of porous crystalline material. It has a periodic multi-dimensional network structure that is formed by the coordination of metal ions or metal cluster units and the self-assemble of organic ligand [12,13]. As the metals and organic ligands can be adjusted and controlled, MOFs exhibit structural diversity and have recently attracted wide attention from the public. Researchers have found that MOFs have potential to be applied in many fields, such as gas storage and separation, catalysis, sensors, drug delivery, etc. [14–17]. In addition, zeolitic imidazolate framework-8 (ZIF-8) is one of the MOFs with outstanding photocatalytic properties, which has been researched many times in the field of photocatalysis. For example, X. Zeng et al. synthesized the TiO_2/ZIF-8 composite, which effectively inhibits the recombination of charge carrier, resulting in an improved photocatalytic activity [18]. Y.H. Ding et al. reported that Bi_2S_3@ZIF-8 core–shell heterostructures exhibited photocatalytic activity to Rhodamine B (RhB) dye degradation under visible light [19]. These results indicated that ZIF-8 based materials have potential applications in the field of photocatalysis.

In this work, a novel Bi_2MoO_6/ZIF-8 composite that displays excellent photocatalytic activity in the degradation of methylene blue (MB) has been successfully synthesized. The nanoparticle of ZIF-8, with different content, has been decorated on the hierarchical flower-like Bi_2MoO_6. The result shows that the Bi_2MoO_6/ZIF-8 composite has excellent photocatalytic performance under visible light.

2. Experimental Section

2.1. Preparation of Bi_2MoO_6

All of the chemicals were of analytical grade and they can be used without further purification. Bi_2MoO_6 powder was prepared by the hydrothermal method [20], $Na_2MoO_4{\cdot}2H_2O$ (1 mmol, 0.4210 g) and $Bi(NO_3)_3{\cdot}5H_2O$ (2 mmol, 1.6866 g) was dissolved in 5 mL ethylene glycol (EG), respectively. After being stirred for 10 min, the above two solutions were mixed together. Subsequently, 20 mL ethanol was added into the above mixture and then stirred for 10 min. Afterwards, the mixture was transferred into a Teflon lined steel autoclave and heated at 160 °C for 20 h. After the autoclave was cooled to room temperature, the yellow products was recovered by filter, washed with deionized water and ethanol, and collected under vacuum at 80 °C for 12 h.

2.2. Preparation of Bi_2MoO_6/ZIF-8 Composites

Figure 1 illustrates the preparation procedure for the Bi_2MoO_6/ZIF-8 composites. In general, the as-synthesized flower-like Bi_2MoO_6 spheres were dispersed into a methanol solution containing 2-methylimidazole (2.4 mmol, 0.66 g), and then stirred for 10 min. $Zn(NO_3)_2{\cdot}6H_2O$ (0.3 mmol 0.03 g) was dispersed into 10 mL methanol. After being stirred for 10 min, the above two solutions were mixed together and stirred for 10 min. The samples were collected by centrifugation (7000 rpm, 5 min), washed by methanol for three times, and finally the Bi_2MoO_6/ZIF-8 composites were dried at 80 °C for 12 h. All of the Bi_2MoO_6/ZIF-8 composites with different molar ratios of Bi_2MoO_6 to 2-methylimidazole (2-MI), i.e., 5:3, 4:3, 3:3, and 2:3, respectively, were also prepared under the similar procedure. The samples were named Bi_2MoO_6/ZIF-8-1, Bi_2MoO_6/ZIF-8-2, Bi_2MoO_6/ZIF-8-3, and Bi_2MoO_6/ZIF-8-4, respectively according to the different molar ratio of Bi_2MoO_6 to 2-MI mentioned above. The syntheses of pure ZIF-8 without Bi_2MoO_6 were prepared in the same way.

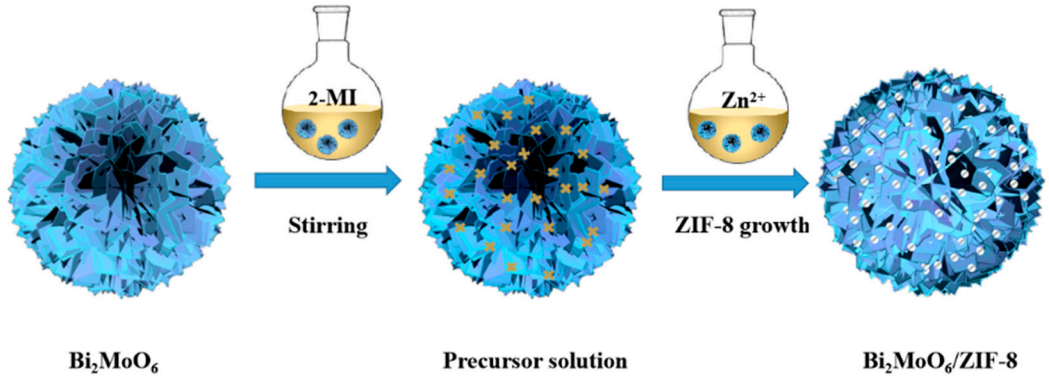

Figure 1. The preparation process of Bi_2MoO_6/ZIF-8 via the self-assembly method.

2.3. Characterization

X-ray powder diffraction (XRD) patterns were obtained from a Karlsruhe D8 Advance powder diffractometer (Bruker, Karlsruhe, Germany) with Cu Kα X-ray radiation (k = 0.15418 nm). A scanning electron microscope (Hitachi SU70, Tokyo, Japan) characterized the morphology images of the Bi_2MoO_6/ZIF-8 composite. Chemical state were analyzed by using X-ray photoelectron spectroscopy (Escalab 250XI, Thermo Fisher Scientific, Waltham, MA, USA).

2.4. Evaluation of Photocatalytic Performance

In this experiment, 20 mg photocatalysts were added to 80 mL aqueous solution of Methylene blue (20 mg/L). To ensure an adsorption/desorption equilibrium, the solution was continuously stirred for 30 min in the dark before light irradiation. Afterwards, turn on the light source, which is made up of 300 W Xe lamps with 420 nm cut-off filters. Take about 4 mL of suspension every 20 min and centrifuge it at the same time. The degradation of methylene blue solution and the UV-visible absorption/diffuse reflectance spectroscopy were characterized by a UV-2450 spectrometer (Shimadzu, Kyoto, Japan).

3. Results and Discussion

3.1. XRD Analysis

Figure 2a shows the X-ray diffraction pattern of simulated ZIF-8, synthesized pure ZIF-8, pure Bi_2MoO_6, and a series of the composite Bi_2MoO_6/ZIF-8-1, Bi_2MoO_6/ZIF-8-2, Bi_2MoO_6/ZIF-8-3, and Bi_2MoO_6/ZIF-8-4. The diffraction peak of the synthesized ZIF-8 conforms to that of the simulated ZIF-8. It indicates that the synthesized samples are pure. The diffraction peak of synthesized Bi_2MoO_6 can be indexed as Bi_2MoO_6 (JCPDS No. 21-0102). Moreover, in Figure 2b, with the increased content of ZIF-8 in the series of composites of Bi_2MoO_6/ZIF-8-(1 to 4), the intensity of the ZIF-8 peak will also be enhanced, but it is not obvious. It is probably because of the low content and crystallinity of ZIF-8 [21]. Subsequent characterization results further support the successful combination of ZIF-8 and Bi_2MoO_6.

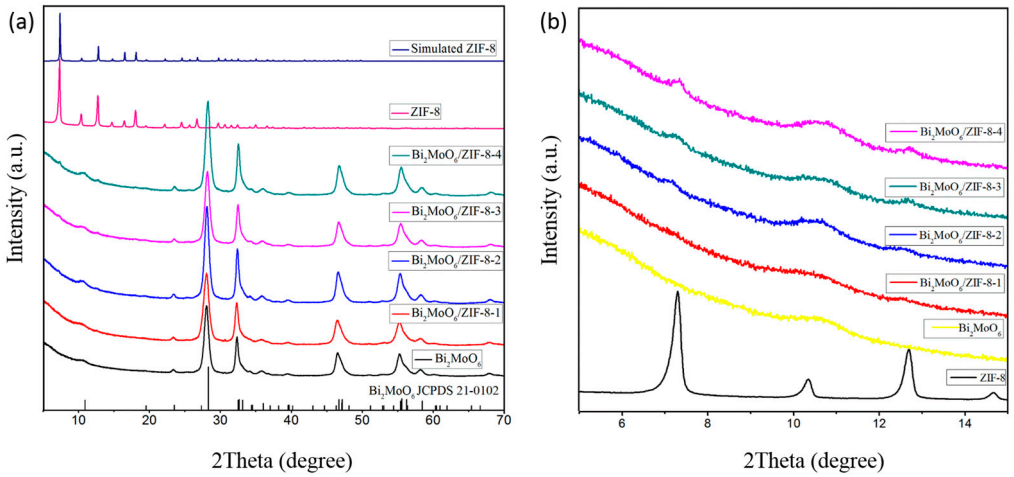

Figure 2. X-ray powder diffraction (XRD) Patterns of simulated zeolitic imidazolate framework-8 (ZIF-8), pure ZIF-8, Bi_2MoO_6, Bi_2MoO_6/ZIF-8-1, Bi_2MoO_6/ZIF-8-2, Bi_2MoO_6/ZIF-8-3, Bi_2MoO_6/ZIF-8-4 (**a**); the magnified XRD pattern of pure ZIF-8, Bi_2MoO_6, Bi_2MoO_6/ZIF-8-1, Bi_2MoO_6/ZIF-8-2, Bi_2MoO_6/ZIF-8-3, Bi_2MoO_6/ZIF-8-4 (**b**).

3.2. Scanning Electron Microscopy (SEM) Analysis

As can be clearly observed in Figure 3a, the SEM image of pure ZIF-8 exhibits regular nanoparticle morphology, with average length about 50 nm. As shown in Figure 3b, the hierarchical flower-like Bi_2MoO_6 spheres with diameter of about 2 μm are composed of many smooth and clean nanosheets. Figure 3c–f shows the morphologies of Bi_2MoO_6/ZIF-8-1, Bi_2MoO_6/ZIF-8-2, Bi_2MoO_6/ZIF-8-3 and Bi_2MoO_6/ZIF-8-4. The amount of ZIF-8 is too small to be observed in Figure 3c. It is obvious that a combination of different content of ZIF-8 is formed on the nanosheets of Bi_2MoO_6 in Figure 3d–f. As the content of ZIF-8 increases, the amount of ZIF-8 on the sheet of Bi_2MoO_6 increases. When the molar ratio of Bi_2MoO_6 to 2-MI is 2:3, Bi_2MoO_6 is wrapped by ZIF-8 and the photocatalytic performance of Bi_2MoO_6/ZIF-8 will also be affected. Figure 4 shows more SEM images of Bi_2MoO_6/ZIF-8-3, which will further demonstrate that the proper amount of ZIF-8 were successfully combined on the Bi_2MoO_6 with an optimal morphology.

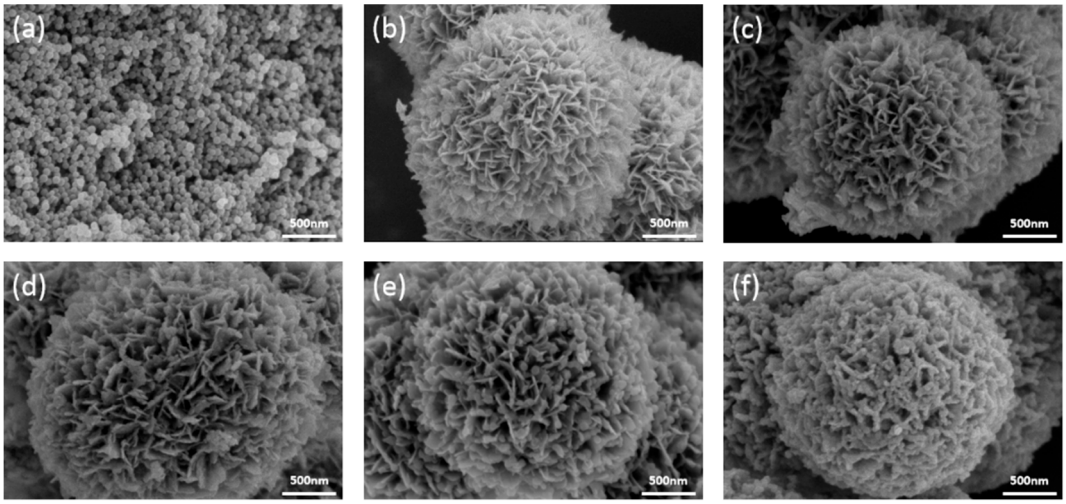

Figure 3. Scanning Electron Microscopy (SEM) image of pure ZIF-8 (**a**), pure Bi_2MoO_6 (**b**), Bi_2MoO_6/ZIF-8-1 (**c**), Bi_2MoO_6/ZIF-8-2 (**d**), Bi_2MoO_6/ZIF-8-3 (**e**), and Bi_2MoO_6/ZIF-8-4 (**f**).

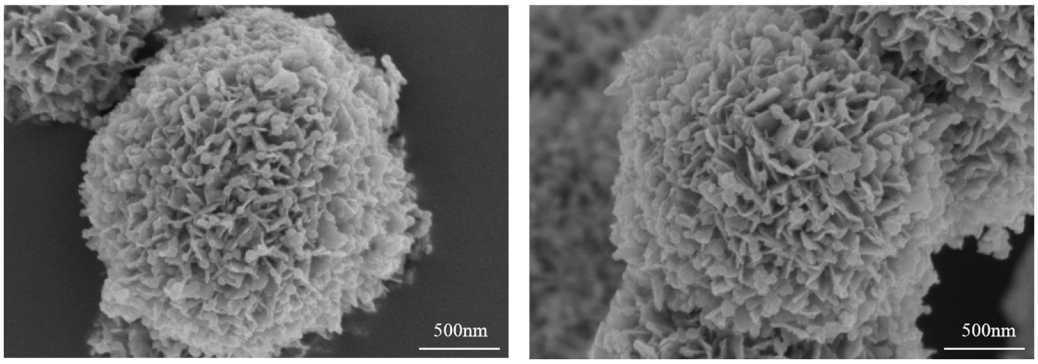

Figure 4. SEM image of Bi_2MoO_6/ZIF-8-3 in different positions.

3.3. X-ray Photoelectron Spectroscopy (XPS) Analysis

The X-ray photoelectron spectroscopy spectrum demonstrates the chemical compositions and the oxidation state of pure Bi_2MoO_6 and Bi_2MoO_6/ZIF-8-3. From the full survey spectrum in Figure 5, it is obvious that a Bi, Mo, O, and C element exits in the sample of pure Bi_2MoO_6. In addition, when compared with pure Bi_2MoO_6, the composite of Bi_2MoO_6/ZIF-8 has two more elements, i.e., Zn and N. In Figure 6a, for the pure Bi_2MoO_6, the two peaks centered at 159.2 eV and 164.6 eV can be ascribed to the Bi $4f_{7/2}$ and Bi $4f_{5/2}$ of Bi^{3+} [22]. In addition, the peaks of Bi_2MoO_6/ZIF-8 composite showed a tiny shift when compared with pure Bi_2MoO_6. In Figure 6b, the two peaks that are centered at 232.6 eV and 235.6 eV correspond to the Mo $3d_{5/2}$ and Mo $3d_{3/2}$ binding energies of Mo^{6+} [23]. For the composites of Bi_2MoO_6/ZIF-8, the binding energy of Mo $3d_{5/2}$ and Mo $3d_{3/2}$ increase 0.4 eV. In Figure 6c, the two peaks that were centered at 1023.3 eV and 1046.2 eV were attributed to the Zn $2p_{3/2}$ and Zn $2p_{1/2}$ of Zn^{2+} in the composites of Bi_2MoO_6/ZIF-8 [24]. These results showed that ZIF-8 has been successfully decorated in Bi_2MoO_6 spheres.

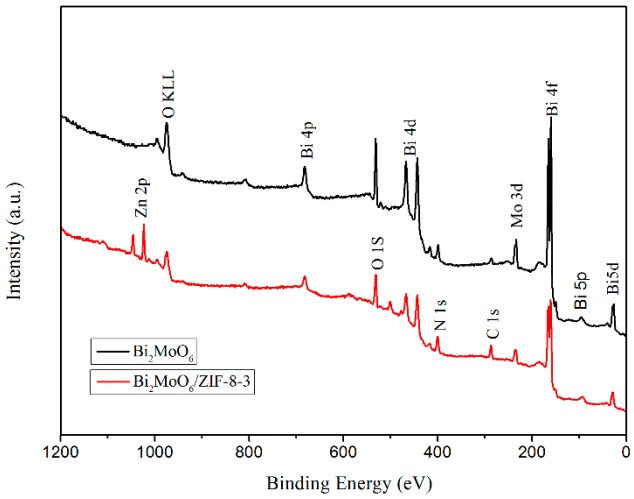

Figure 5. Survey X-ray photoelectron spectroscopy (XPS) spectrum of pure Bi_2MoO_6 and Bi_2MoO_6/ZIF-8-3.

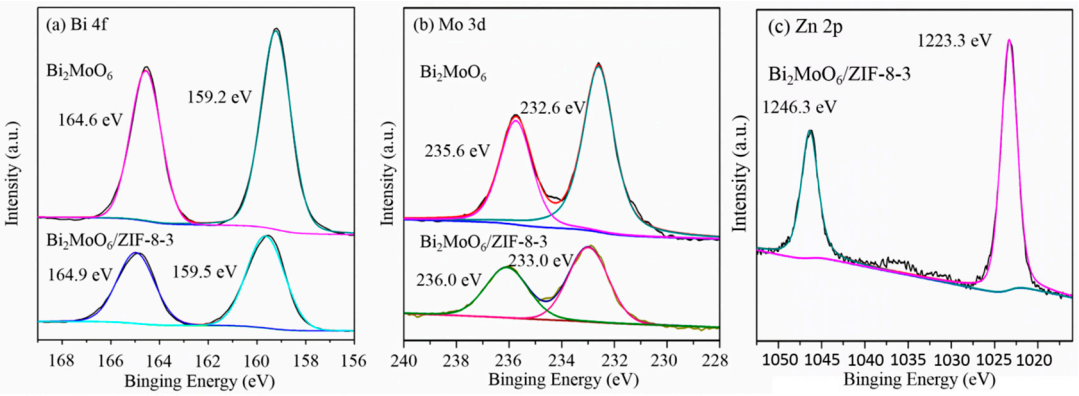

Figure 6. Survey XPS spectrum of pure Bi_2MoO_6 and Bi_2MoO_6/ZIF-8-3, high-resolution spectrum of Bi 4f (**a**), Mo 3d (**b**), and Zn 2p (**c**).

3.4. Photocatalytic Activities

As shown in Figure 7a, the degradation of MB under the visible light irradiation determined the photocatalytic degradation activities of different photocatalysts. The MB photodegradation rate of pure Bi_2MoO_6 is 47.89% and that of pure ZIF-8 is 34.05%. When the composite is Bi_2MoO_6/ZIF-8-3, the degradation of MB increased to 66.88%. From the time dependent UV–vis spectrum changes of MB catalyzed by Bi_2MoO_6/ZIF-8-3, as shown in Figure 7b, it is obvious that it has excellent adsorption performance and photocatalytic performance. In addition, the photocatalytic performance of the composite of Bi_2MoO_6/ZIF-8 is improved when compared with that of the pure Bi_2MoO_6. Therefore, ZIF-8 plays an important role in the degradation process. In the first three groups of composites (Bi_2MoO_6/ZIF-8-(1 to 3)), the photocatalytic performance of the composite gradually increases with the increase of photocatalysts content. Continuing to increase the content of ZIF-8 will reduce its performance, which is possibly due to the fact that the generation of exceeding ZIF-8 on the sheet of Bi_2MoO_6 inhibited its absorption of light. This phenomenon also corresponds to the results of the previous SEM.

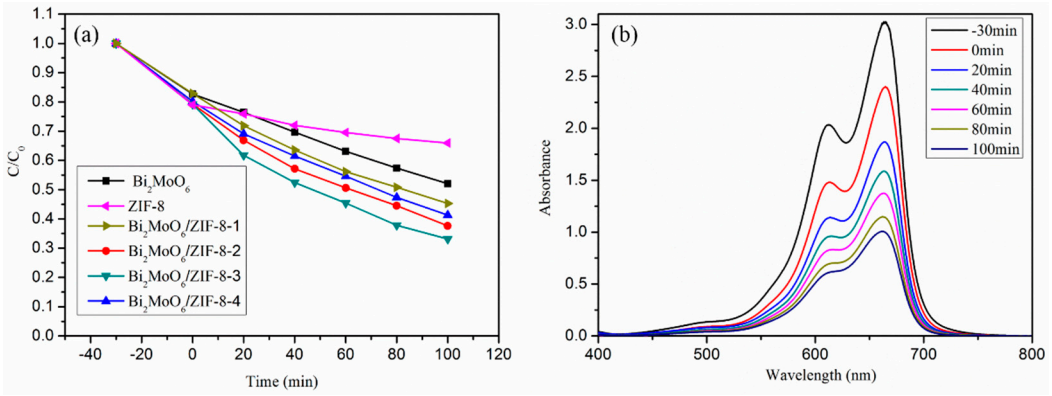

Figure 7. The photocatalytic degradation efficiencies of different photocatalysts to degrade methylene blue (MB) (**a**); Time dependent UV–vis spectrum changes of MB catalyzed by Bi_2MoO_6/ZIF-8-3 (**b**).

Accordingly, in order to understand the photocatalytic mechanism of these composites, a possible mechanism for the photocatalytic degradation of MB over Bi_2MoO_6/ZIF-8 composites is proposed. In the Bi_2MoO_6/ZIF-8 composites, the conduction band (CB) and valence band (VB) of Bi_2MoO_6 are −0.32 eV and 2.34 eV [25] and the CB and VB of ZIF-8 are −3.41 eV and 1.68 eV [24]. Under the irradiation of the light source, Bi_2MoO_6 is more prone to generating the photogenerated electron-hole pair and the VB of Bi_2MoO_6 is more positive than that of ZIF-8, the photogenerated hole that is generated by Bi_2MoO_6 would transfer the VB of ZIF-8, which would promote the separation of electron-hole pairs and improve the photocatalytic performance of the composite.

4. Conclusions

In summary, a series of Bi_2MoO_6/ZIF-8 composites with a different content of ZIF-8 have been successfully fabricated by a facile self-assembly method. The photocatalysts of Bi_2MoO_6/ZIF-8 have better performance than pure Bi_2MoO_6 in the degradation of MB under the visible light. The successful composition of ZIF-8 and Bi_2MoO_6 inhibited the recombination of a photogenerated electron–hole pair. When the molar ratio of Bi_2MoO_6 to 2-MI is 3:3, the amount of ZIF-8 that is decorated on flower-like Bi_2MoO_6 is suitable and the ability of photocatalysis would reach the maximum. This composing strategy of Bi_2MoO_6/ZIF-8 would provide a new route in the designing of highly efficient visible light photocatalysts.

Author Contributions: Conceptualization, Y.-y.L.; formal analysis, Y.X. and S.-k.S.; writing—original draft preparation, Y.X.; writing—review and editing, Y.-y.L.; supervision, X.-r.Z. and J.Z.; funding acquisition, Y.-y.L.

Funding: This work was financially supported by the National Natural Science Foundation of China (Grant No. 51702218), National Natural Science Foundation of Guangdong, China (Grant No. 2016A030310054 and 2017A030310009), and Opening Funding of State Key Laboratory of New Ceramics and Fine Processing, School of Materials Science and Engineering of Tsinghua University (Grant No. KF201601).

Acknowledgments: This work was financially supported by the National Natural Science Foundation of China (Grant No. 51702218), National Natural Science Foundation of Guangdong, China (Grant No. 2016A030310054 and 2017A030310009), and Opening Funding of State Key Laboratory of New Ceramics and Fine Processing, School of Materials Science and Engineering of Tsinghua University (Grant No. KF201601).

Conflicts of Interest: The authors declare no conflict of interest.

References

1. Yue, D.T.; Qian, X.F.; Zhao, Y.X. Photocatalytic remediation of ionic pollutant. *Sci. Bull.* **2015**, *60*, 1791–1806. [CrossRef]
2. Si, Y.H.; Xia, Y.; Shang, S.K.; Xiong, X.B.; Zeng, X.R.; Zhou, J.; Li, Y.Y. Enhanced visible light driven photocatalytic behavior of $BiFeO_3$/ Reduced Graphene Oxide composites. *Nanomaterials* **2018**, *8*, 526. [CrossRef] [PubMed]
3. Shang, L.; Tong, B.; Yu, H. CdS Nanoparticle-decorated Cd nanosheets for efficient visible light-driven photocatalytic hydrogen evolution. *Adv. Energy Mater.* **2016**, *6*, 1501241–1501247. [CrossRef]
4. Devi, L.G.; Kavitha, R. A review on nonmetal ion doped titania for the photocatalytic degradation of organic pollutants under UV/solar light: Role of photogenerated charge carrier dynamics in enhancing the activity. *Appl. Catal. B Environ.* **2013**, *140*, 559–587. [CrossRef]
5. Shimodaira, Y.; Kato, H.; Kobayashi, H.; Kudo, A. Photophysical properties and photocatalytic activities of bismuth molybdates under visible light irradiation. *J. Phys. Chem. B* **2006**, *110*, 17790–17797. [CrossRef] [PubMed]
6. Tian, G.H.; Chen, Y.J.; Zhou, W.; Pan, K.; Dong, Y.Z. Facile solvothermal synthesis of hierarchical flower-like Bi_2MoO_6 hollow spheres as high performance visible-light driven photocatalysts. *J. Mater. Chem.* **2011**, *21*, 887–892. [CrossRef]
7. Li, S.J.; Shen, X.F.; Liu, J.S.; Zhang, L.S. Synthesis of Ta_3N_5/Bi_2MoO_6 core-shell fiber shaped heterojunctions as efficient and easily recyclable photocatalysts. *Environ. Sci. Nano* **2017**, *4*, 1155–1167. [CrossRef]
8. Li, X.X.; Fang, S.M.; Ge, L.; Han, C.C.; Qiu, P.; Liu, W.L. Synthesis of flower-like Ag/AgCl-Bi_2MoO_6 plasmonic photocatalysts with enhanced visible-light photocatalytic performance. *Appl. Catal. B Environ.* **2015**, *176*, 62–69. [CrossRef]
9. Wang, M.; Han, J.; Guo, P.Y.; Sun, M.Z.; Zhang, Y.; Tong, Z.; You, M.Y.; Lv, C.M. Hydrothermal synthesis of B-doped Bi_2MoO_6 and its high photocatalytic performance for the degradation of Rhodamine B. *J. Phys. Chem. Solids* **2018**, *113*, 86–93. [CrossRef]
10. Wang, D.J.; Shen, H.D.; Guo, L.; Wang, C.; Fu, F.; Liang, Y.C. Ag/Bi_2MoO_6-x with enhanced visible-light-responsive photocatalytic activities via the synergistic effect of surface oxygen vacancies and surface plasmon. *Appl. Surf. Sci.* **2018**, *436*, 536–547. [CrossRef]

11. Liu, D.; Wang, J.; Wang, Y.G.; Zhu, Y.F. An anion exchange strategy for construction of a novel Bi_2SiO_5/Bi_2MoO_6 heterostructure with enhanced photocatalytic performance. *Catal. Sci. Technol.* **2018**, *8*, 3278. [CrossRef]
12. Jiang, H.L.; Makal, T.A.; Zhou, H.C. Interpenetration control in metal-organic frameworks for functional applications. *Chem. Rev.* **2013**, *257*, 2232–2249. [CrossRef]
13. Farha, O.K.; Hupp, J.T. Rational design, synthesis, purification, and activation of metal-organic framework materials. *Acc. Chem. Res.* **2010**, *43*, 1166–1175. [CrossRef] [PubMed]
14. Li, J.R.; Kuppler, R.J.; Zhou, H.C. Selective gas adsorption and separation in metal-organic frameworks. *Chem. Soc. Rev.* **2009**, *38*, 1477–1504. [CrossRef] [PubMed]
15. Ke, F.; Wang, L.; Zhu, J. Facile fabrication of CdS-metal-organic framework nanocomposites with enhanced visible-light photocatalytic activity for organic transformation. *Nano Res.* **2015**, *8*, 1834–1846. [CrossRef]
16. Lu, Z.Z.; Zhang, R.; Li, Y.Z. Solvatochromic behavior of a nanotubular metal-organic framework for sensing small molecules. *J. Am. Chem. Soc.* **2011**, *133*, 4172–4174. [CrossRef]
17. An, J.Y.; Gei, S.J.; Rosi, N.L. Cation-Triggered Drug Release from a Porous Zinc-Adeninate Metal-Organic Framework. *J. Am. Chem. Soc.* **2009**, *131*, 8376–8377. [CrossRef]
18. Zeng, X.; Huang, L.Q.; Wang, C.N.; Wang, J.S.; Li, J.T.; Luo, X.T. Sonocrystallization of ZIF-8 on electrostatic spinning TiO_2 nanofibers surface with enhanced photocatalysis property through synergistic effect. *ACS Appl. Mater. Interfaces* **2016**, *8*, 20274–20282. [CrossRef] [PubMed]
19. Ding, Y.H.; Zhang, X.L.; Zhang, N.; Zhang, J.Y.; Zhang, R.; Liu, Y.F.; Fang, Y.Z. A visible-light driven Bi_2S_3@ZIF-8 core-shell heterostructure and synergistic photocatalysis mechanism. *Dalton Trans.* **2018**, *47*, 684–692. [CrossRef]
20. Zhang, J.L.; Liu, H.; Ma, Z. Flower-like Ag_2O/Bi_2MoO_6 p-n heterojunction with enhanced photocatalytic activity under visible light irradiation. *J. Mol. Cata. A Chem.* **2016**, *424*, 37–44. [CrossRef]
21. Venna, S.R.; Jasinski, J.B.; Carreon, M.A. Structural evolution of zeolitic imidazolate framework-8. *J. Am. Chem. Soc.* **2010**, *132*, 18030–18033. [CrossRef] [PubMed]
22. Liu, Y.; Yang, Z.H.; Song, P.P.; Xu, R.; Wang, H. Facile synthesis of $Bi_2MoO_6/ZnSnO_3$ heterojunction with enhanced visible light photocatalytic degradation of methylene blue. *Appl. Surf. Sci.* **2018**, *430*, 561–570. [CrossRef]
23. Xia, K.X.; Chen, H.X.; Mao, M.; Chen, Z.G.; Xu, F.; Yi, J.J.; Yu, Y.H.; She, X.J. Designing visible-light-driven z-Scheme catalyst 2D g-C_3N_4/Bi_2MoO_6: Enhanced photodegradation activity of organic pollutants. *Phys. Status Solidi A* **2018**, *215*, 1800520. [CrossRef]
24. Liu, X.; Zhang, J.; Dong, Y.M.; Li, H.X.; Xia, Y.M.; Wang, H.J. A facile approach for the synthesis of Z-scheme photocatalyst ZIF-8/g-C_3N_4 with highly enhanced photocatalytic activity under simulated sunlight. *New J. Chem.* **2018**, *42*, 12180–12187. [CrossRef]
25. Zhang, M.Y.; Shao, C.L.; Mu, J.B.; Zhang, Z.Y.; Guo, Z.C.; Zhang, P.; Liu, Y.C. One-dimensional Bi_2MoO_6/TiO_2 hierarchical heterostructures with enhanced photocatalytic activity. *CrystEngComm* **2012**, *14*, 605–612. [CrossRef]